The Plant Cell, Vol. 16, 1790–1800, July 2004, www.plantcell.org © 2004 American Society of Plant Biologists

Efficient Assembly of Photosystem II in *Chlamydomonas reinhardtii* Requires Alb3.1p, a Homolog of Arabidopsis ALBINO3

Friedrich Ossenbühl,[a] Vera Göhre,[b] Jörg Meurer,[a] Anja Krieger-Liszkay,[c] Jean-David Rochaix,[b] and Lutz A. Eichacker[a,1]

[a] Department for Biology I, Ludwig-Maximilians-University Munich, D-80638 Munich, Germany
[b] Departments of Molecular Biology and Plant Biology, University of Geneva, CH-1211 Geneva 4, Switzerland
[c] Institute for Biology II, Biochemistry of Plants, University of Freiburg, D-79104 Freiburg, Germany

Alb3 homologs Oxa1 and YidC have been shown to be required for the integration of newly synthesized proteins into membranes. Here, we show that although Alb3.1p is not required for integration of the plastid-encoded photosystem II core subunit D1 into the thylakoid membrane of *Chlamydomonas reinhardtii*, the insertion of D1 into functional photosystem II complexes is retarded in the *Alb3.1* deletion mutant *ac29*. Alb3.1p is associated with D1 upon its insertion into the membrane, indicating that Alb3.1p is essential for the efficient assembly of photosystem II. Furthermore, levels of nucleus-encoded light-harvesting proteins are vastly reduced in *ac29*; however, the remaining antenna systems are still connected to photosystem II reaction centers. Thus, Alb3.1p has a dual function and is required for the accumulation of both nucleus- and plastid-encoded protein subunits in photosynthetic complexes of *C. reinhardtii*.

INTRODUCTION

The targeting and translocation of proteins into and/or across the thylakoid membrane involves at least four different pathways inside the chloroplast. Each of these pathways uses a specific set of protein factors and has specific energy requirements (Keegstra and Cline, 1999). Some proteins enter the membrane without any obvious requirements for protein or energy factors (Schleiff and Klosgen, 2001), whereas others use the bacterial related cpSec or cpTAT/ΔpH pathways (Mori and Cline, 2001). The cpSec pathway uses a translocase comprising cpSecY and cpSecE in the thylakoid membranes and a stromal factor cpSecA acting as a piston to translocate the substrate through the translocon. This function is ATP dependent and can be stimulated by a ΔpH across the thylakoid membrane. The cpTAT/ΔpH pathway uses three thylakoid membrane proteins, Hcf106, cpTatC, and Tha4, and strictly requires a ΔpH across the thylakoid membranes in vitro, whereas recent in vivo data obtained with *Chlamydomonas reinhardtii* show no ΔpH dependence of the cpTAT/ΔpH pathway (Finazzi et al., 2003).

The proteins of the light-harvesting complexes are transported via the cpSRP pathway into the thylakoid membranes (Eichacker and Henry, 2001). This pathway uses the stromal proteins cpSRP54 and cpSRP43, which bind as heterodimers or heterotrimers to the imported LHCPs forming the so-called transit complex. The membrane insertion of the LHCPs strictly requires cpFtsY, GTP, and the integral membrane protein Alb3 in vitro (Tu et al., 1999; Moore et al., 2000, 2003). However, disruption of the genes encoding cpSRP54 and cpSRP43 in *Arabidopsis thaliana* has only mild effects on the accumulation of LHCPs in comparison with the wild type, whereas the disruption of Alb3p leads to a loss of LHCPs (Sundberg et al., 1997; Tu et al., 1999; Hutin et al., 2002). This suggests the existence of an alternative insertion pathway of LHCPs into the thylakoid membrane and/or additional functions of the mutated factors in vivo. It is only for cpSRP54 that an additional role could be demonstrated for the cotranslational targeting/membrane insertion of D1, a reaction center protein of photosystem II (PSII; Nilsson et al., 1999).

The nuclear gene encoding chloroplast Alb3p was identified by complementation of an *albino* mutant (*alb3*) of Arabidopsis. The albino phenotype of the *alb3* mutant is severe with strongly reduced thylakoid membranes and almost no granal structures. It is likely that this *alb3* phenotype is not only the result of the loss of LHCP integration into thylakoid membranes, and it suggests additional functions for Alb3p (Sundberg et al., 1997).

Alb3p belongs to a widespread protein family with homologs in all organisms examined. Members of this protein family appear to be involved in the integration and/or assembly of membrane proteins (Kuhn et al., 2003). Besides Alb3p, which is localized in thylakoid membranes, chloroplasts of Arabidopsis contain an Alb3 homolog, Artemis (Fulgosi et al., 2002). Artemis consists of an N-terminal receptor domain and a C-terminal Alb3 domain. It is localized in the inner envelope membrane and is required for organellar division. Interestingly, the only Alb3p homolog in the unicellular cyanobacterium *Synechocystis* sp PCC 6803 is also

[1] To whom correspondence should be addressed. E-mail eichacker@lmu.de; fax 0049-89-17861209.
The author responsible for distribution of materials integral to the findings presented in this article in accordance with the policy described in the Instructions for Authors (www.plantcell.org) is: Lutz A. Eichacker (eichacker@lmu.de).
Article, publication date, and citation information can be found at www.plantcell.org/cgi/doi/10.1105/tpc.023226.

involved in cell division, although it lacks the N-terminal receptor domain present in Artemis (Fulgosi et al., 2002).

Recently, two nuclear genes encoding the Alb3p homologs Alb3.1p and Alb3.2p were characterized in *C. reinhardtii* (Bellafiore et al., 2002). The *Alb3.1* gene was cloned, and the protein function was characterized by complementation of a nuclear mutant, *ac29.* The *Alb3.2* gene was identified through a homology search of the EST database of *C. reinhardtii* with the sequence of Alb3.1p. Both genes lack an N-terminal receptor domain, suggesting that they are involved in LHCP integration into thylakoids. This is supported by the phenotype of *ac29*, which still accumulates ~10% LHCPs in comparison with the wild type and is therefore significantly weaker than the *alb3* phenotype in Arabidopsis (Sundberg et al., 1997). Thus, it was postulated that Alb3.2p can partially complement the lack of Alb3.1p in *ac29* (Bellafiore et al., 2002).

The best analyzed examples of Alb3p homologs are the mitochondrial Oxa1p and the bacterial YidCp (Kuhn et al., 2003). Oxa1p is required for the integration of nucleus- and mitochondria-encoded proteins into the inner mitochondrial membrane (Hell et al., 2001), whereas the bacterial YidCp is involved in the cotranslational insertion of inner membrane proteins. The YidC protein has recently been proposed to also be required for the assembly of inserted membrane proteins by cleaning the SecYEG translocase (Chen et al., 2002). Interestingly, the *ΔyidC* mutant of *Escherichia coli* can be complemented by the *Alb3* gene of Arabidopsis, thus pointing to a common function (Jiang et al., 2002).

Here, we show that loss of Alb3.1p affects the assembly of PSII in the *C. reinhardtii* mutant *ac29*. Although the reaction center protein D1 is apparently integrated normally into the thylakoid membrane, insertion of D1 into PSII is retarded. Coimmunoprecipitation experiments reveal that Alb3.1p interacts with full-length D1, indicating that Alb3.1p operates as a membrane integral chaperone in an early step of PSII assembly.

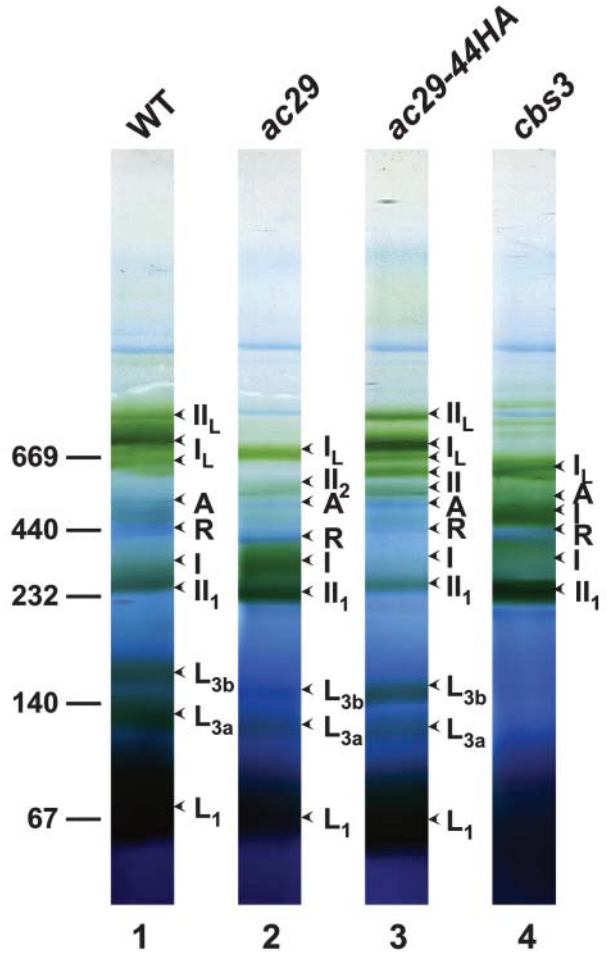

Figure 1. BN-PAGE of Membranes from Wild-Type, *ac29*, *ac29-44HA*, and *cbs3* Cells.

Membranes of wild-type (1), *ac29* (2), *ac29-44HA* (3), and *cbs3* cells (4) were solubilized and separated by a BN-PAGE (see Methods). Arrows indicate the position of complexes containing PSI-LHCI (I_L), PSI (I), PSII-LHCII (II_L), PSII RCC dimer (II_2), PSII RCC monomer (II_1), ATP synthase (A), Rubisco (R), and monomeric (L_1) and trimeric (L_{3a} and L_{3b}) light-harvesting complex proteins of PSII, respectively. The molecular masses of standard protein complexes are given in kD.

RESULTS

In *ac29*, Light-Harvesting Proteins Are Coupled to Reaction Center Protein Complexes

The *Alb3.1* gene is disrupted in the *C. reinhardtii* mutant *ac29*. This mutation leads to an ~90% loss of nucleus-encoded light-harvesting proteins (LHCP) of PSI and PSII. In addition, the level of plastid-encoded PSII reaction center proteins (RC) is reduced by 50% during growth in the light (Bellafiore et al., 2002). These results indicate that Alb3.1p is required for the integration and/or assembly of the nucleus- and plastid-encoded PSII proteins in the thylakoid membrane. To characterize the assembly state of protein complexes in wild-type and *ac29* cells, complexes were separated by blue native (BN) gel electrophoresis (Figure 1). Protein subunits of the complexes were then identified by mass spectrometry after separation of subunits in a second dimension by SDS-PAGE (data not shown).

In *ac29*, four changes in protein complex composition relative to the wild type were readily observed: (1) no PSII-LHCII supercomplexes (II_L) were present; (2) ~90% of PSI reaction center complexes (I) were not connected with LHCI proteins (I_L); (3) the yield of monomeric PSII reaction center core (RCC; II_1) was decreased, whereas dimeric RCC (II_2) was increased; and (4) the overall amount of LHCII (L_1, L_{3a}, and L_{3b}) was decreased to ~10% (Figure 1, lanes 1 and 2). To verify the absence of PSII-LHCII supercomplexes in *ac29*, we increased the sensitivity for detection of proteins in two-dimensional (2D)-BN/SDS-PAGE by coupling the fluorescent dye Cy2 to Lys residues of native thylakoid membrane proteins via an NHS ester. Moreover, the functional state of LHCII coupling to PSII RCC was analyzed by 77K fluorescence spectroscopy in vivo (Figure 2). To test for coupling of LHCII with RC complexes, the *C. reinhardtii* mutant *Δycf9* was used as a control because it had been shown in

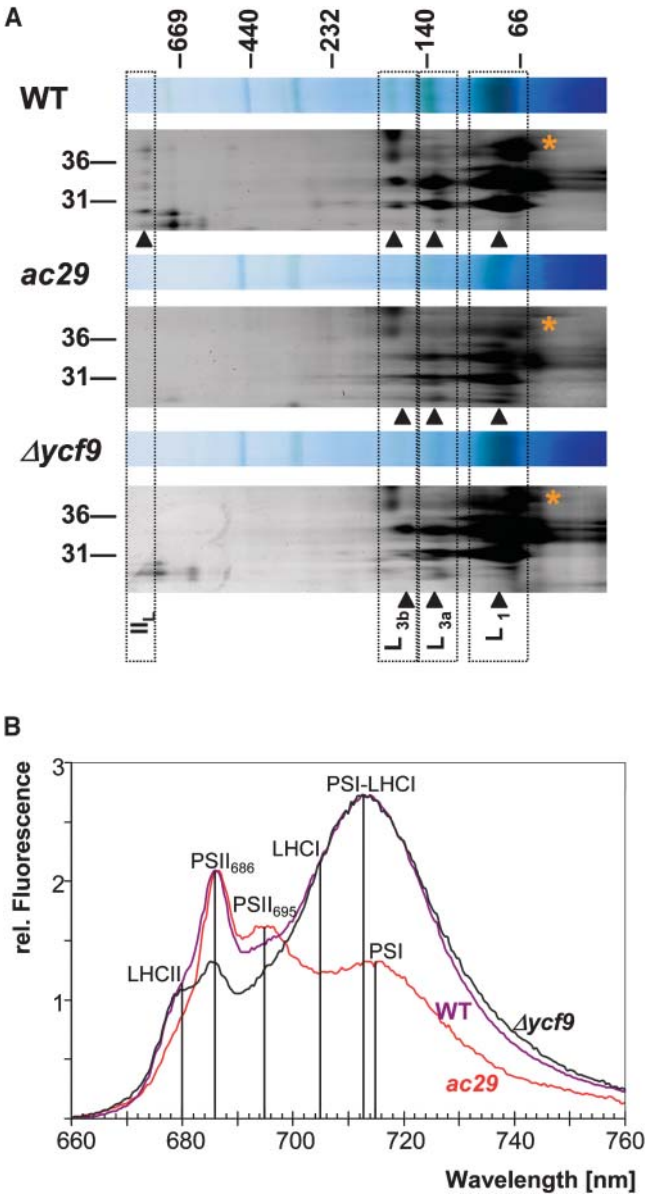

Figure 2. BN-PAGE and Fluorography of Chromophores Bound to Membrane Proteins.

(A) Membranes labeled with fluorescent dye from wild-type, *ac29*, and *Δycf9* cells were solubilized and proteins separated by BN-PAGE (top) and 2D-BN/SDS-PAGE (bottom). The position of CP26 is marked by an asterisk; dotted frames mark the position of complexes containing LHCII (Figure 1). The molecular masses of standard protein complexes are given in kD.

(B) The 77K fluorescence emission spectra of wild-type (violet), *ac29* (red), and *Δycf9* (dark gray) cells. Protein complexes corresponding to the emission maxima are labeled in the figure body (PSI and PSI-LHCI; $PSII_{686}$ and $PSII_{695}$; LHCI and LHCII, light-harvesting complexes of PSI and PSII, respectively).

tobacco (*Nicotiana tabacum*) plants that the absence of PsbZ (Ycf9) results in the loss of LHCII coupling to the PSII RCC (Swiatek et al., 2001).

The results showed that all LHCII monomers and trimeric LHCII complexes were present in the wild type, *ac29*, and *Δycf9*. However, only ~10% of the major LHCPs and only ~2% of the CP26 protein were found in *ac29*, whereas no difference in the amount of LHCII protein level was observed in *Δycf9* in comparison with the wild type (Figure 2A, L_1, L_{3a}, L_{3b}, and asterisks). In the high molecular mass PSII-LHCII fraction, LHCII was only found in wild-type cells representing ~10% of the total LHCII content (Figure 2A, II_L). Because we could not rule out the possibility that PSII-LHCII supercomplexes solubilized from membranes might be unstable during BN-PAGE, we compared the connection of LHCII with RC complexes in all three strains by 77K fluorescence spectroscopy in vivo (Figure 2B). In *Δycf9*, the LHCII fluorescence yield at 680 nm was comparable to that of the wild type when spectra were normalized at the PSI-LHCI peak. However, the fluorescence yield from PSII RCC proteins at 686 nm was only ~60% of the corresponding wild-type peaks. This indicated that the energy transfer from LHCII to PSII RCC and, thereby, the fluorescence emission from PSII were decreased in *Δycf9.* In *ac29*, the fluorescence yield from PSI-LHCI complexes at 715 nm was decreased, most likely because of the low level of LHCI and PSI-LHCI complexes (Figure 2B, compare also Figure 1). Also, fluorescence emission from LHCII at 680 nm was low as a consequence of the low LHCII level. However, when we normalized the *ac29* spectrum to the PSII-CP43 emission at 686 nm of the wild-type spectrum, fluorescence emission from CP47 at 695 nm was higher relative to wild-type cells. Excitation of the inner antenna proteins CP43 and CP47 largely depends on the energy transfer from LHCII complexes. This therefore indicated that LHCII proteins are functionally coupled to the PSII reaction center and that fluorescence emission from CP47 is favored in *ac29*.

Because the *ac29* mutant grows slowly photoautotrophically, we analyzed the functionality of PSII in *ac29* by thermoluminescence and pulse amplitude-modulated room temperature chlorophyll fluorescence measurements (PAM; Figure 3). In thermoluminescence, the emitted light originates from charge recombination of trapped charges (Vass and Inoue, 1992). The charge pairs involved can be identified by their emission temperature, which depends on the redox potentials of the charge pair. The most important charge pair measured in thermoluminescence of PSII is the recombination of the S2 or S3 state of the oxygen-evolving complex at the donor side with the second electron accepting semiquinone of PSII (Q_B) at the acceptor side, which yields the B-band at ~30°C (Rutherford et al., 1982). Thermoluminescence measurements reveal two bands, the B-band and the afterglow band (Ducruet and Miranda, 1992; Krieger et al., 1998). We applied an increasing number of exciting single turnover flashes on dark-adapted *C. reinhardtii* cells and analyzed the intensity oscillation of the B-band (Figure 3A). In the wild type, the highest intensity of the B-band was observed after the second flash, indicating that the plastoquinone pool is largely reduced in these algae. The intensity of this band oscillates with a period of four. In *ac29*, the intensity of the B-band was lowered by ~50%, and the oscillation pattern was strongly attenuated but comparable to the wild type. This indicated the presence of

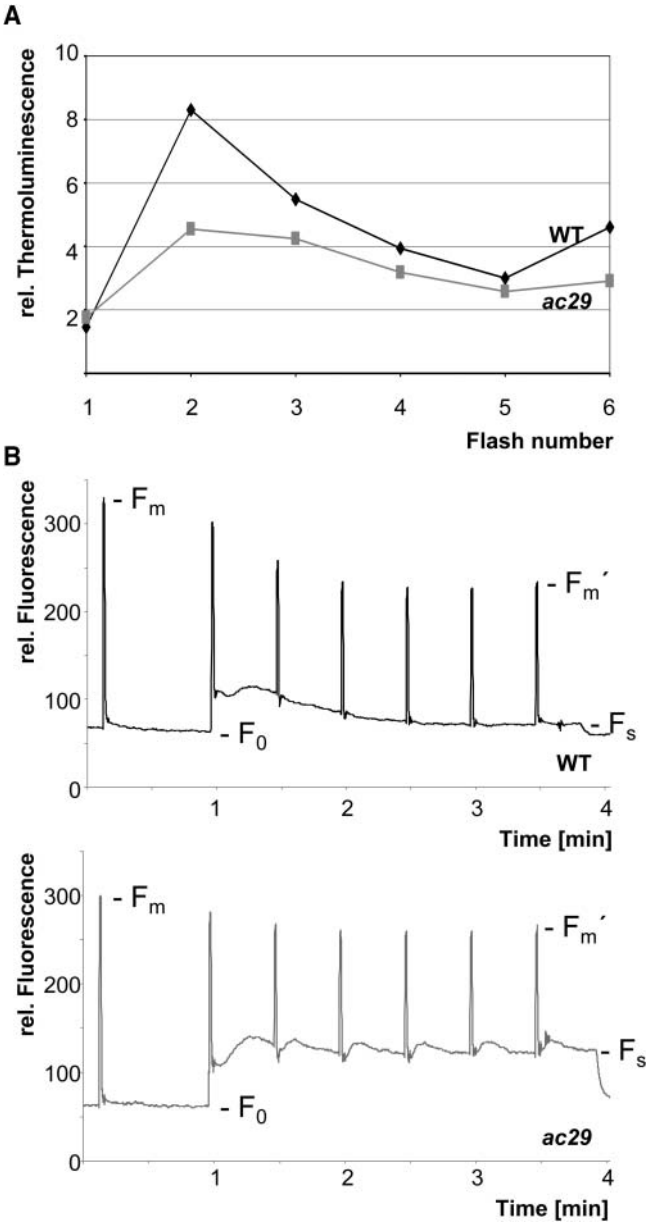

Figure 3. Thermoluminescence and PAM Fluorometry of Wild-Type and *ac29* Cells.

(A) Flash number–dependent B-band oscillation of charge recombination in PSII was measured by thermoluminescence of dark-adapted wild-type (closed) and *ac29* cells (shaded) of *C. reinhardtii* (see Methods).
(B) Induction and photochemical quenching kinetics of chlorophyll fluorescence (PAM) of wild-type (top) and *ac29* (bottom) cells were performed as described in Methods. The minimal (F_o), steady state (F_s), and maximal fluorescence yields (F_m and F_m' under actinic light, respectively) are indicated.

a lower but functional amount of PSII in *ac29* without major differences in its electron transport ability in comparison with the wild type.

Because our data indicated that electron transport in PSII was not blocked in *ac29*, we investigated next whether the slow photoautotrophic growth could result from electron transport constrains between PSII and PSI. The photosynthetic quantum yield of dark-adapted PSII was determined by PAM (Krause and Weis 1991). A F_v/F_m ratio of 0.79 $\pm$ 0.02 and 0.80 $\pm$ 0.03 was measured in *ac29* and wild-type cells, respectively, confirming that PSII function is not affected (Figure 3B). However, steady state fluorescence (F_s) was significantly increased in *ac29* as compared with the wild type. After six flashes under actinic light, photochemical quenching was close to 1.0 in the wild type but only 0.70 $\pm$ 0.05 in *ac29.* These data indicate that electron efflux from PSII is limited in the mutant. We therefore conclude that the *ac29* phenotype could result from loss of LHCI coupling to PSI. A low quantum yield for PSI-driven electron transport could lead to the observed accumulation of Q_A^-, which may lead to donor side photoinhibition of PSII and increased PSII turnover. We therefore investigated the de novo synthesis and stability of RCC subunits in *ac29* and wild-type cells in vivo.

Accumulation of PSII Reaction Center Protein D1 Is Diminished in *ac29*

Turnover of PSII is best studied by radiolabeling of the plastid encoded RC subunit D1. The D1 protein turns over rapidly in PSII complexes, and assembly of the de novo synthesized protein can be followed with high sensitivity by 2D-BN/SDS-PAGE. Radiolabeling of thylakoid membrane proteins in wild-type and *ac29* cells revealed three major signals: the D1 protein, the α-subunit and the β-subunit of the ATP synthase, AtpA, and AtpB, respectively (Figure 4). The radiolabel kinetics of AtpA showed two similar phases in wild-type and *ac29* cells: a start-up phase with highest radiolabel accumulation during the first 5 min and a slower phase of continued radiolabel accumulation when cells were incubated further (Figure 4, lanes 1 to 5 and 7 to 11, AtpA). A similar labeling pattern was found for D1 in wild-type cells (Figure 4, lanes 1 to 5, D1). However, when the radiolabeling kinetics of D1 was quantified in *ac29* cells, two characteristic changes were apparent. Compared with the wild type, the start-up phase was slower, and there was no further increase in labeling of D1 after 10 min (Figure 4, lanes 7 to 11, D1). To test whether the labeling of the D1 protein was low because of an increased degradation rate in *ac29* cells, we tested the stability of the AtpA and D1 proteins in wild-type and *ac29* cells (Figure 4, lanes 6 and 12). At least 90% of the proteins labeled for 15 min were stable over 60 min, indicating that the stability of the synthesized AtpA and D1 proteins was not significantly different in the wild type and *ac29.* To analyze integration of the D1 protein into the thylakoid membrane, we quantified the amount of D1 in the soluble and the total membrane phase of wild-type and *ac29* cells. The amount of radiolabeled D1 protein in the soluble phase was only 10% of D1 in the membrane fractions for both wild-type and *ac29* cells (Figure 5A). Also, D1 could not be extracted from the membrane with 100 mM sodium carbonate, pH 11.0, whereas the peripheral AtpA protein was readily extracted (Figure 5B). Furthermore, trypsin digestion of in vivo radiolabeled membranes generated similar degradation products in the wild type and *ac29* (Figure 5C). Taken together, these results strongly suggest that the D1 protein is normally integrated in the mutant. Thus, it appears that the insertion of D1 in the PSII RC complex is

affected in the mutant rather than the integration of D1 into the membrane. We therefore analyzed next how de novo expressed D1 protein assembles into PSII.

Assembly of the Reaction Center Protein D1 into the PSII RC Is Retarded in *ac29*

In the wild type, assembly of the D1 protein into RCC(1) is rapid. After a 15-min pulse, highest incorporation of radiolabel was detected in RCC(1) without concomitant radiolabel accumulation in membrane-inserted but unassembled D1 protein (free protein; Figure 6, wild-type lane 15′). This radiolabel distribution was observed when pulses were as short as 5 min (data not shown). Prolonged pulse and pulse-chase labeling experiments furthermore demonstrated that RCC(1) is the major site of D1 accumulation, corroborating that D1 is stable in RCC(1) complexes and that assembly of dimeric RCC- and PSII-LHCII complexes from RCC(1) is slow (Figure 6, wild-type lane 75′ and 15′/60′). By contrast, when the assembly kinetics of de novo expressed D1

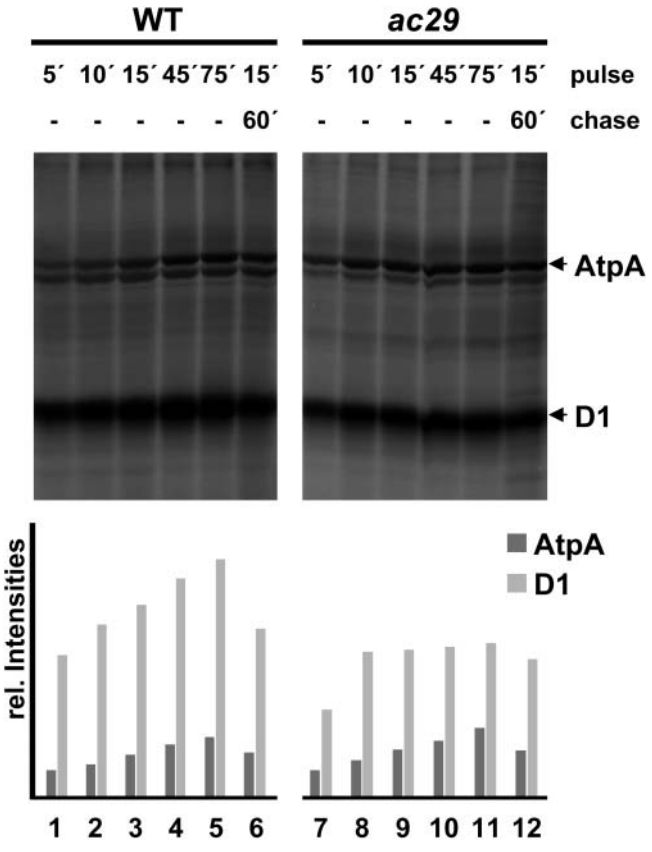

Figure 4. Autoradiography of Membrane Proteins Isolated from Radiolabeled Wild-Type and *ac29* Cells.

Wild-type (lanes 1 to 6) and *ac29* (lanes 7 to 12) cells (2×10^6) were pulse radiolabeled with [^{35}S]sulfate in vivo for 5, 10, 15, 45, and 75 min (lanes 1 to 5 and 7 to 11) or pulse labeled for 15 min and chased for additional 60 min (lanes 6 and 12). Proteins were separated by SDS-PAGE. Quantification of D1 and AtpA radiolabeling (rel. Intensities) of lanes 1 to 12 is plotted below the autoradiograph.

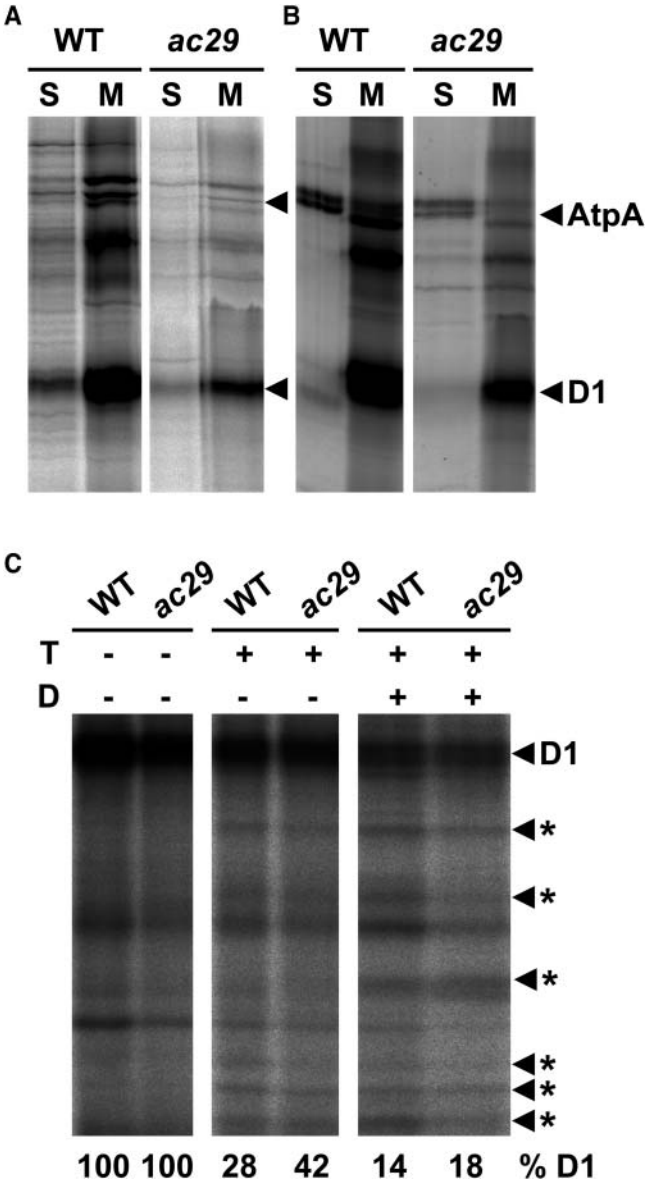

Figure 5. Autoradiography of Pulse-Radiolabeled Proteins from Wild-Type and *ac29* Cells.

(A) Wild-type and *ac29* cells (2×10^6) were pulse radiolabeled with [^{35}S]sulfate in vivo for 15 min. Proteins of the soluble (S) and total membrane (M) phases were separated by SDS-PAGE.

(B) Total membranes from wild-type and *ac29* cells (described in **[A]**) were incubated with 100 mM sodium carbonate and centrifuged. Proteins from the supernatant (S) and the membrane phase (M) were separated by SDS-PAGE. Arrows point to radiolabeled D1 and AtpA, respectively.

(C) Total membranes from wild-type and *ac29* cells (described in **[A]**) were incubated for 30 min at 25°C in the absence (−) or presence (+) of trypsin (T) and β-dodecylmaltoside (D). Percentages of remaining full-length D1 (%D1) in relation to the controls are given under each lane.

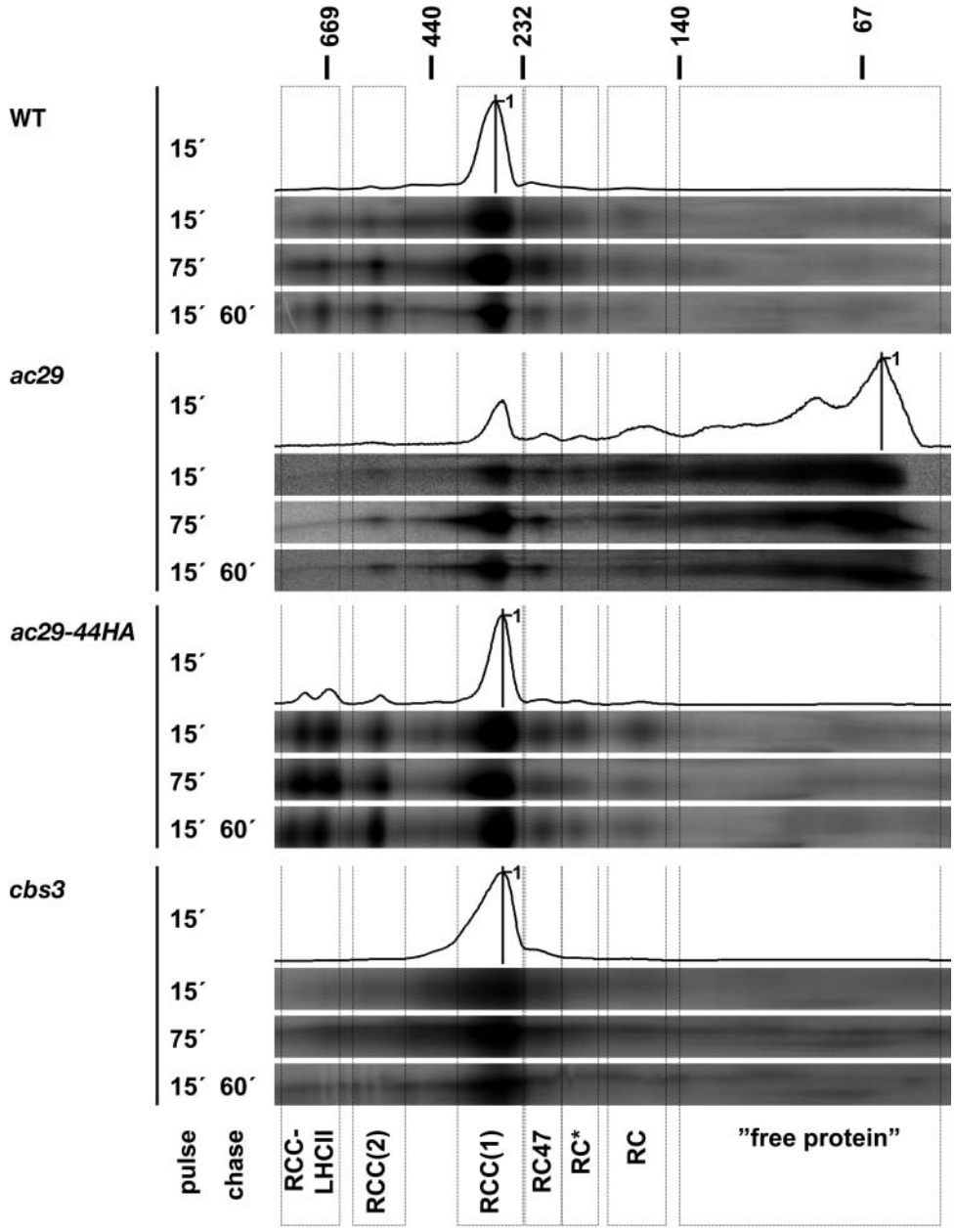

Figure 6. Autoradiography of Membrane Proteins Isolated from Radiolabeled Wild-Type, *ac29*, *ac29-44HA*, and *cbs3* Cells.

Wild-type, *ac29*, *ac29-44HA*, and *cbs3* cells (2×10^6) were pulse and pulse-chase labeled with [^{35}S]sulfate in vivo as described (Figure 4). Membranes were separated by 2D-BN/SDS-PAGE. Complexes containing radiolabeled D1 protein are presented in a molecular mass window as indicated in kD for BN-PAGE. D1 radiolabeling after 15-min pulse labeling was quantified across the BN-PAGE window, and each spectrum was normalized to the highest peak. Frames (dotted lines) highlight the position of PSII-assembly complexes [RC; RC* reaction center complexes of PSII including D1 and D2; RC47 reaction center complex of PSII including CP47; RCC(1) and RCC(2), monomeric and dimeric RCC complexes of PSII; RCC-LHCII, RCC plus LHCII complexes; free protein, unassembled protein solubilized from the membrane phase].

protein was analyzed in *ac29* cells, the majority of the D1 protein was maintained in the free protein fraction, although assembly of the RCC(1) and RCC(2) complexes was not blocked. Prolonged pulse and pulse-chase radiolabeling then clearly revealed that assembly of the D1 protein into the RCC(1) complex is slow in *ac29* cells (Figure 6, *ac29*, lanes 75′ and 15′/60′). Quantification of the radiolabel distribution in unassembled and assembled D1 revealed that during the 60-min chase, D1 assembled into PSII complexes, but the protein was not degraded, indicating that stability of the D1 protein is high in *ac29* (Figure 6, *ac29*, lanes 75′

and 15′/60′). We therefore conclude that the assembly of the D1 protein into the monomeric RCC complex is retarded in *ac29* as compared with wild-type cells and that unassembled D1 in *ac29* is highly stable. These data suggested that the rate-limiting step for D1 assembly in the wild type could be de novo expression of the D1 protein, whereas in *ac29*, accumulation of membrane-inserted D1 protein in RC complexes (Figure 6, RC and RC*) is rate limiting, indicating that Alb3.1p is operating at an early step of PSII assembly. However, the data did not exclude that the retarded D1 assembly is an indirect effect of the decreased accumulation of LHC proteins. We therefore investigated whether the absence of LHCP influences the rate of D1 assembly in RCC(1) complexes.

The Defect in D1 Assembly in *ac29* Is Not Because of the Reduced LHCII Level

Defective D1 assembly in *ac29* could be a direct consequence of the loss of the Alb3.1p function or an indirect effect of the reduced level of light-harvesting proteins. To test the influence of LHCP accumulation on D1 assembly, we analyzed the *ac29* strain complemented with the *Alb3.1* gene (*ac29-44HA*; Bellafiore et al., 2002) and a mutant strain lacking chlorophyll *b* because of a loss of the chlorophyll *a* oxygenase gene (*cbs3*; Tanaka et al., 1998). In *ac29-44HA*, PSII-LHCII and PSI-LHCI complexes were restored, and the amount of protein complexes were comparable to wild-type levels (Figure 1, lane 3). When *cbs3* was analyzed by BN-PAGE, no chlorophyll-containing LHCII complexes were detectable (Figure 1, lane 4). However, after separation of the protein complexes into corresponding subunits by SDS-PAGE, chlorophyll-free LHCII proteins were released from the low molecular mass region of the BN gel, and the proteins were identified by mass spectrometry (data not shown). Only minor amounts of LHCI were detected in complexes with PSI as well, whereas the amount of PSII exclusively found as RCC(1) was significantly increased (Figure 1, lane 4).

The accumulation of D1 in *ac29-44HA* and *cbs3* was unaffected because D1 radiolabeling and the AtpA signal increased in parallel in both strains, and also the stability of both proteins was not impaired (data not shown). Moreover, the assembly kinetics of D1 into the monomeric RCC was unchanged in *ac29-44HA* and *cbs3* compared with the wild type, and no free D1 protein accumulated in both strains. It was, however, remarkable that the assembly of PSII stopped at the level of RCC(1) in *cbs3* (Figure 6). These data revealed that the assembly defect of D1 in *ac29* was completely restored in *ac29-44HA* and, furthermore, that the lack of functional LHCII complexes did not influence D1 assembly. We therefore conclude that the retarded assembly of D1 in *ac29* is not a secondary effect as a result of the reduced LHCP level but results directly from the lack of Alb3.1p.

Interactions between Alb3.1p and D1

The observation that assembly of D1 into RCC(1) is retarded in the *Alb3.1*-deficient *ac29* mutant raises the possibility that full-length D1 and Alb3.1p interact with each other. To test this possibility, thylakoid membranes from the *ac29* strain were complemented with hemagglutinin (HA) epitope tagged Alb3.1p, and membranes were solubilized to be used for reciprocal coimmunoprecipitations with D1 and HA antisera. As negative control, membranes from a strain containing an unrelated HA-tagged protein were used. Using an α-HA affinity matrix and solubilized membranes, D1 was coimmunoprecipitated in extracts from two independent transformants expressing Alb3.1-HA (Figure 7A; data not shown). No D1 protein could be detected when the immunoprecipitation was performed with membranes from the control strain. Similarly, immunoprecipitation with D1 antiserum revealed the presence of Alb3.1-HA. The specificity was tested by performing the same immunoprecipitation with extracts from the control strain containing the unrelated HA-tagged protein. Under these conditions, D1 was undetectable (Figure 7B). We therefore conclude that Alb3.1p and D1 interact, although it is not yet known whether this interaction is direct or indirect.

DISCUSSION

In this study, we report that Alb3.1p is not only involved in the integration of LHCPs into the thylakoid membrane but also acts

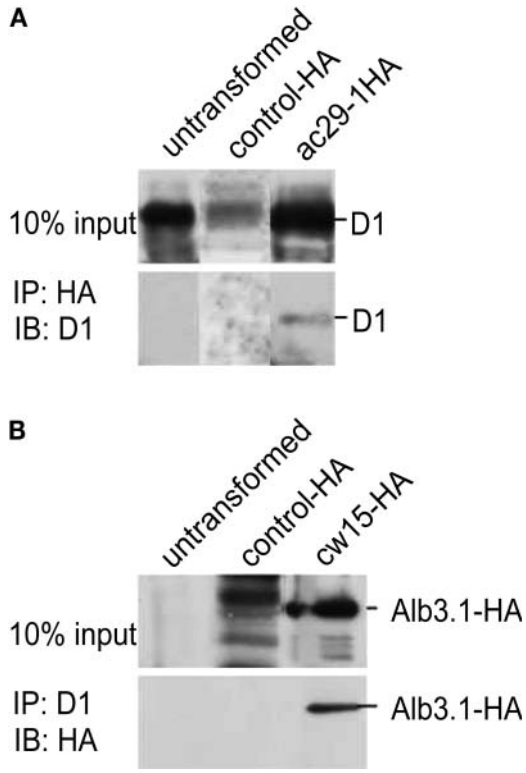

Figure 7. Interaction of Alb3.1p with D1.

Membranes from strains containing the HA-tagged Alb3.1 (ac29-1HA, cw15-HA), an unrelated HA-tagged control protein (control-HA), or no HA-tagged protein (untransformed) were solubilized as described in Methods. Immunoprecipitations (IP) were performed using HA antiserum **(A)** or D1 antiserum **(B)**. Ten percent of the solubilized membranes (top panels) and the immunoprecipitated proteins (bottom panels) were analyzed by immunoblotting (IB) with D1 antisera **(A)** and HA antisera **(B)**.

as a catalyst during assembly of D1 into the PSII reaction center of *C. reinhardtii*. We show that accumulation of D1 in PSII is significantly reduced in mutant *ac29* cells. Nevertheless, PSII is fully functional in the mutant. In addition, we demonstrate by comparison with the mutants *cbs3* and *Δycf9* that D1 accumulation in *ac29* is not affected by a reduced level of LHCII, thus indicating at least two distinct functions of Alb3.1p in LHCP integration and D1 assembly.

No functional LHCII complexes could be detected in *cbs3* by BN-PAGE, although detectable levels of LHCP accumulated. This was already shown earlier (Polle et al., 2000), and similar results were obtained for another chlorophyll *b*–less mutant of *C. reinhardtii*, *cbn1-113* (Park and Hoober, 1997). However, these data differ from those of higher plants, in which disruption of the chlorophyll *a* oxygenase gene in Arabidopsis does not eliminate the expression of the LHCP genes but leads to a complete loss of LHCPs (Espineda et al., 1999; J. Meurer, unpublished data). Because we detected a higher expression rate of LHCPs in Arabidopsis than in *C. reinhardtii*, the difference might result from a faster degradation of nonfunctional LHCPs in higher plants (data not shown). Spectroscopic studies of *cbs3* however showed that the PSII antenna is functional (Polle et al., 2000). The presence of antenna chlorophyll molecules remains to be clarified, but from our data, it is unlikely that PSII contains LHCPs in *cbs3*.

Analysis of mutants *cbs3* and *Δycf9* revealed that assembly of PSII RCC(1) and of LHCII complexes are not linked. In *cbs3*, RCC(1) assembles in the absence of functional LHCPs, whereas in *Δycf9*, stable PSII assembles, even though no LHCII antenna can attach to the complexes RCC(1) or RCC(2) (Swiatek et al., 2001). Therefore, we conclude that the reduced amount of LHCPs and the retarded assembly of the D1 protein are distinct aspects of the *ac29* phenotype.

During BN-PAGE, PSII-LHCII supercomplexes appear to be unstable because in BN gels of the wild type, only ~10% of LHCII is attached to PSII, whereas the residual LHCII is detectable as monomers and trimers. Because of the reduced LHCII level in *ac29*, it is therefore not surprising that no PSII-LHCII supercomplex is detectable in this mutant. However, 77K fluorescence emission data indicate that the LHCII complexes present in *ac29* are attached to PSII RCC complexes in vivo. PSII displays two fluorescence emission peaks at 695 nm and 686 nm corresponding to CP47 and CP43, respectively (Alfonso et al., 1994; Shen and Vermaas, 1994). In *ac29*, the CP47 peak was significantly higher as compared with the CP43 peak than in the wild type, indicating a higher energy transfer to CP47 than to CP43 and attachment of a higher number of antennae proteins to CP47 than to CP43. This conclusion agrees with a three-dimensional structural model of PSII, in which an attachment of the trimeric LHCII complexes was proposed to occur via CP29 and CP24 to CP47 and via CP26 and PsbZ to CP43 (Eckardt, 2001). Because CP26 is the subunit that is reduced the most among the chlorophyll binding proteins in *ac29*, the amount of LHCII complexes attached to CP43 should be lower than those attached to CP47. This may explain the diminished fluorescence emission from CP43. The reason for the decrease in CP26 compared with the other LHCPs in *ac29* is not clear. The different LHCPs may use separate alternative integration pathways. Alb3.2p, a second homolog of Alb3, was previously considered to perform the residual LHCP integration into thylakoids as a result of a partially redundant function with Alb3.1p (Bellafiore et al., 2002). Hence, decreased membrane insertion of CP26 would be specifically because of the loss of Alb3.1p.

In our in vivo labeling experiments in the wild type and *ac29*, assembly intermediates revealed identical molecular mass PSII complexes, suggesting that functional assembly occurs in both strains. Functionality of PSII was furthermore demonstrated by fluorescence and thermoluminescence measurements and by the ability of *ac29* to grow photoautotrophically. Integration of radiolabeled D1 in wild-type and *ac29* membranes was shown to be undistinguishable as judged from base extraction and trypsin digestion of membranes. However, despite the correct D1 integration into the thylakoid membrane, assembly of D1 into the PSII RC of *ac29* was less efficient as a result of the loss of Alb3.1p. This protein is the homolog of mitochondrial Oxa1p and of bacterial YidC, which have been described as integrases involved in the translocation and/or integration of membrane proteins (Moore et al., 2000, 2003; Kuhn et al., 2003). Nevertheless, it was reported that the integral membrane Cox3p and Pf3 coat protein integrate into membranes independently from Oxa1p and YidC, respectively, although with a lower integration efficiency (Hell et al., 2001; Serek et al., 2004).

Because in vivo pulse-chase labeling revealed that accumulation but not stability of D1 was affected in *ac29*, it is possible that a regulatory feedback loop exists between accumulation of unassembled D1 and its synthesis. If assembly of D1 into PSII complexes is retarded as found for *ac29*, free D1 protein is expected to accumulate in the thylakoid membrane. This unassembled D1 protein could downregulate its own translation in a similar way as proposed for the CES process (control by epistasy of synthesis; Choquet et al., 1998). In this case the synthesis of cytochrome *f* is regulated through the assembly state of the cytochrome b_6f complex. Low amounts of free cytochrome *f* can block its own synthesis indirectly at the level of translation initiation presumably by interacting with a *trans*-acting factor. Similar mechanisms have been proposed for the ordered assembly of other photosynthetic complexes of the thylakoid membrane, including PSII (Choquet and Wollman, 2002). However, in the case of the *ac29* mutant, this regulatory feedback loop remains to be confirmed because we cannot rule out the possibility that the accumulation of membrane integral and unassembled D1 may lead to a higher turnover of de novo synthesized D1 protein in *ac29*, which would have remained undetected by our in vivo labeling approach.

Integration of D1 into the thylakoid membrane has been described as cotranslational event that involves three different steps. After initiation of the D1 translation, cpSRP54 interacts with the nascent peptide chain to target the ribosome *psbA* mRNA complex (RNCs) to the thylakoid membrane (Nilsson et al., 1999). A receptor for the cpSRP54-RNC complex in the thylakoid membrane has not yet been identified, although cpFtsY has been proposed as candidate. During integration in the membrane, the ribosome-bound nascent D1 peptide interacts with the cpSecY translocase and with D2 for assembly (Zhang et al., 2001). However, several additional steps have to be performed for functional integration and assembly. Alb3.1p could facilitate the

release of D1 from the translocase, promote an interaction of D1 with D2, support correct folding, or provide cofactors for folding. The last two functions might converge with the involvement of Alb3.1p as a membrane integral chaperone during integration of LHCP into the membrane because chlorophyll cofactors are essential for the correct and stable integration of LHCP and the D1 protein in the membrane.

METHODS

Strains and Media

The *Chlamydomonas reinhardtii* wild-type strain 137c and the mutant strains *ac29*, *ac29-44HA* (Bellafiore et al., 2002), *cbs3* (Tanaka et al., 1998), and *Δycf9* (Swiatek et al., 2001) were maintained on Tris-acetate-phosphate (TAP) medium (Gorman and Levine, 1965) at 25°C and 40 μE m^{-2} s^{-1}.

Membrane Extraction and Gel Electrophoresis

Cultures were grown in TAP medium to a density of 2 × 10^6 cells/mL. Cells were harvested by centrifugation at 6000*g* for 10 min and resuspended in 500 μL of TMK buffer (10 mM Tris/HCl, pH 6.8; 10 mM $MgCl_2$; 20 mM KCl) to a density of 5 × 10^6 cells/mL. All further steps were performed on ice or at 4°C. Altogether 0.3 g of glass beads (100 to 200 μm) were added to the cells, and the suspension was agitated twice for 1 min on a Vortex mixer with an intermediate cooling on ice for at least 2 min. The supernatant was removed and the glass beads were washed at least three times with 250 μL of TMK. The collected and combined supernatants were centrifuged at 16,000*g* for 5 min. The sedimented membranes were resuspended in 80 μL of ACA buffer (750 mM ε-aminocaproic acid; 50 mM Bis-Tris, pH 7.0; 0.5 mM EDTA) and solubilized by adding β-dodecylmaltoside to a final concentration of 1% and incubating on ice 10 min. The unsolubilized material was removed by centrifugation at 16,000*g* for 10 min. Five microliters of loading solution (750 mM ε-aminocaproic acid; 5% Coomassie Brilliant Blue G 250) was added to the supernatant before loading the BN polyacrylamide gradient gels. BN gel electrophoresis was performed at 12 mA constant current as described (Schagger and von Jagow, 1991). For the second dimension (so-called 2D-BN/SDS gels), a single lane of the BN gel was solubilized in solubilization buffer (66 mM Na_2CO_3; 100 mM β-mercaptoethanol; 2% SDS) and loaded on a 12.5% SDS-polyacrylamide gel containing 4 M urea (Laemmli, 1970). The 2D-BN/SDS gels were run overnight at 16 mA constant current and 15°C.

To analyze the integration of membrane proteins, isolated total membranes were washed with 100 mM sodium carbonate and centrifuged at 16,000*g* for 10 min. For protease treatment, isolated total membranes were incubated for 30 min at room temperature in the absence or presence of 10 μg/mL of trypsin or 10 μg/mL of trypsin and 1% β-dodecylmaltoside. The resulting samples were analyzed on a 12.5% SDS-polyacrylamide gel containing 4 M urea (Laemmli, 1970).

Fluorescence Labeling of Thylakoid Membranes

Isolated thylakoid membranes corresponding to 3 × 10^6 cells from *C. reinhardtii* were resuspended in 80 μL of TMK buffer, pH 8.5. For labeling, 0.16 μL of Cy2 solution (Amersham Biosciences, Freiburg, Germany) were added, and the suspension was incubated for 30 min on ice in the dark. The labeling reaction was stopped by addition of 1 μL of a 10 mM Lys solution and further incubated for 10 min on ice. The labeled thylakoid membranes were sedimented by centrifugation and used for 2D-BN/SDS gel electrophoresis as described before. The fluorescent dye was detected in the unstained gels with a Typhoon 9400 variable mode imager (Amersham Biosciences).

77K Fluorescence Spectroscopy

C. reinhardtii cultures (2 × 10^6 cells/mL) were adjusted to 20% glycerol and frozen in liquid nitrogen. The 77K fluorescence spectroscopy was performed with a LS55 luminescence spectrometer using FL Winlab software (Perkin-Elmer, Buckinghamshire, UK) and an excitation light with a wavelength of $\lambda = 430$ nm.

Thermoluminescence Measurements

Thermoluminescence was measured on *C. reinhardtii* cultures (2 × 10^6 cells/mL) with a home-built apparatus (Krieger et al., 1998). PSII was excited with single turnover flashes at 0°C. The flashes were spaced with a 1-s dark interval. Samples were then heated with a heating rate of 20°C/min to 70°C, and the light emission was recorded. Graphical and numerical data analyses were performed according to Ducruet and Miranda (1992).

Fluorometric Studies

Chlorophyll *a* fluorescence measurements were performed in a cuvette using a density of 2 × 10^6 cells/mL in TAP medium with a commercial pulse amplitude-modulated fluorometer PAM 101 interphased with the PAM data acquisition system PDA-100 (Walz, Effeltrich, Germany). Cells were dark adapted for 5 min before the fluorescence measurements. The minimal (F_o), steady state (F_s), and maximal (F_m) fluorescence yield and the variable fluorescence, F_v, calculated as $F_m - F_o$, as well as the ratio F_v/F_m, which reflects the potential yield of the photochemical reaction of PSII, were recorded at 20°C. Photochemical and nonphotochemical quenching, qP and NPQ, respectively, were calculated according to van Kooten and Snel (1990). The intensity of the actinic light was 50 μE m^{-2} s^{-1} and that of the saturating light flash (1 s) used for detection of F_m and the maximal fluorescence during induction, F_m', was 7000 μE m^{-2} s^{-1}.

In Vivo Labeling of *C. reinhardtii*

In vivo labeling of *C. reinhardtii* with [^{35}S] was performed as described previously (Nickelsen et al., 1999). For the pulse/chase analysis, the medium containing [^{35}S] was replaced after 15 min by nonradioactive medium, and the incubation was prolonged for 60 min. After labeling, membranes were isolated from 90% of the samples and analyzed on 2D-BN/SDS gels as described above. The residual 10% of the samples were solubilized in SDS loading buffer (200 mM Na_2CO_3; 100 mM β-Mercaptoethanol; 6% SDS; 30% sucrose; 0.09% bromphenol blue) and loaded on a 12.5% SDS-polyacrylamide gel containing 4 M urea. After the electrophoresis (see above), the gels were stained with Coomassie Brilliant Blue R 250, dried, and exposed to phosphor imaging plates (Fuji Photo Film [Europe], Cologne, Germany). The imaging plates were read out with a FLA3000 image reader and quantified with the supplied AIDA software (Raytest Isotopenmessgeräte, Straubenhardt, Germany).

Coimmunoprecipitations

Membranes were extracted as described and diluted to a final concentration of 0.8 mg chlorophyll/mL in ACA buffer. All further steps were performed at 4°C. For solubilization β-dodecylmaltoside was added to 0.5 mg of chlorophyll per reaction at a final concentration of 0.9%. After incubation on ice for 30 min, unsolubilized material was removed by centrifugation at 12,000*g* for 10 min at 4°C. For immunoprecipitation of the HA epitope, 50 μL per reaction of anti-HA affinity matrix (Sigma, Taufkirchen, Germany) were prepared according to the manufacturer's

instructions and added to 0.3 mg of chlorophyll of solubilized membranes. Binding was performed overnight at 4°C. For immunoprecipitation of D1, 10 μL of D1 antiserum was added to 0.3 mg of chlorophyll of solubilized membranes for each strain. Binding was performed overnight at 4°C. Twenty microliters of Protein-G agarose beads (Roche, Mannheim, Germany) were prepared according to the manufacturer's instructions and added to the solubilized membranes containing the D1 antibody. Binding was performed for 2 h at 4°C. All beads were washed six times in TBS (100 mM Tris/HCl, pH 7.5, 150 mM NaCl), and the bound proteins were eluted in 40 μL 2× SDS loading dye (100 mM Tris/HCl, pH 6.8, 4% SDS, 0.2% bromophenol blue, 20% glycerol) for 30 min at room temperature. Thirty microliters of solubilized membranes and immunoprecipitated proteins were analyzed by immunoblotting with HA or D1 antibodies.

ACKNOWLEDGMENTS

We thank Ayumi Tanaka (*cbs3*) and Francis-Andre Wollman (*Δycf9*) for providing mutant strains and Veronika Reisinger and Bernhard Granvogl for help with the Cy2 labeling and the mass spectrometry, respectively. This work was supported by the Deutsche Forschungsgemeinschaft (SFB 594, Teilprojekt B9) and the Swiss National Foundation (Grant 3100-0667763.02).

Received April 5, 2004; accepted April 16, 2004.

REFERENCES

Alfonso, M., Montoya, G., Cases, R., Rodriguez, R., and Picorel, R. (1994). Core antenna complexes, CP43 and CP47, of higher plant photosystem II. Spectral properties, pigment stoichiometry, and amino acid composition. Biochemistry **33,** 10494–10500.

Bellafiore, S., Ferris, P., Naver, H., Gohre, V., and Rochaix, J.-D. (2002). Loss of Albino3 leads to the specific depletion of the light-harvesting system. Plant Cell **14,** 2303–2314.

Chen, M., Xie, K., Jiang, F., Yi, L., and Dalbey, R.E. (2002). YidC, a newly defined evolutionarily conserved protein, mediates membrane protein assembly in bacteria. Biol. Chem. **383,** 1565–1572.

Choquet, Y., Stern, D.B., Wostrikoff, K., Kuras, R., Girard-Bascou, J., and Wollman, F.A. (1998). Translation of cytochrome f is autoregulated through the 5′ untranslated region of *petA* mRNA in *Chlamydomonas* chloroplasts. Proc. Natl. Acad. Sci. USA **95,** 4380–4385.

Choquet, Y., and Wollman, F.A. (2002). Translational regulations as specific traits of chloroplast gene expression. FEBS Lett. **529,** 39–42.

Ducruet, J.M., and Miranda, T. (1992). Graphical and numerical analysis of thermoluminescence and fluorescence emission in photosynthetical material. Photosynth. Res. **33,** 15–27.

Eckardt, N.A. (2001). A role for PsbZ in the core complex of photosystem II. Plant Cell **13,** 1245–1248.

Eichacker, L.A., and Henry, R. (2001). Function of a chloroplast SRP in thylakoid protein export. Biochim. Biophys. Acta **1541,** 120–134.

Espineda, C.E., Linford, A.S., Devine, D., and Brusslan, J.A. (1999). The *AtCAO* gene, encoding chlorophyll a oxygenase, is required for chlorophyll b synthesis in *Arabidopsis thaliana*. Proc. Natl. Acad. Sci. USA **96,** 10507–10511.

Finazzi, G., Chasen, C., Wollman, F.A., and de Vitry, C. (2003). Thylakoid targeting of Tat passenger proteins shows no delta pH dependence *in vivo*. EMBO J. **22,** 807–815.

Fulgosi, H., Gerdes, L., Westphal, S., Glockmann, C., and Soll, J. (2002). Cell and chloroplast division requires ARTEMIS. Proc. Natl. Acad. Sci. USA **99,** 11501–11506.

Gorman, D.S., and Levine, R.P. (1965). Cytochrome f and plastocyanin, their sequence in the photosynthetic electron transport chain of *Chlamydomonas reinhardi*. Proc. Natl. Acad. Sci. USA **54,** 1665–1669.

Hell, K., Neupert, W., and Stuart, R.A. (2001). Oxa1p acts as a general membrane insertion machinery for proteins encoded by mitochondrial DNA. EMBO J. **20,** 1281–1288.

Hutin, C., Havaux, M., Carde, J.P., Kloppstech, K., Meiherhoff, K., Hoffman, N., and Nussaume, L. (2002). Double mutation cpSRP43-/cpSRP54--is necessary to abolish the cpSRP pathway required for thylakoid targeting of the light-harvesting chlorophyll proteins. Plant J. **29,** 531–543.

Jiang, F., Yi, L., Moore, M., Chen, M., Rohl, T., van Wijk, K.J., de Gier, J.W., Henry, R., and Dalbey, R.E. (2002). Chloroplast YidC homolog Albino3 can functionally complement the bacterial YidC depletion strain and promote membrane insertion of both bacterial and chloroplast thylakoid proteins. J. Biol. Chem. **277,** 19281–19288.

Keegstra, K., and Cline, K. (1999). Protein import and routing systems of chloroplasts. Plant Cell **11,** 557–570.

Krause, G.H., and Weis, E. (1991). Chlorophyll fluorescence and photosynthesis: The Basics. Annu. Rev. Plant Physiol. Plant Mol. Biol. **42,** 313–349.

Krieger, A., Bolte, S., Dietz, K.J., and Ducruet, J.M. (1998). Thermoluminescence studies on the facultative crassulacean-acid-metabolism plant Mesembryanthemum crystallinum L. Planta **205,** 587–594.

Kuhn, A., Stuart, R., Henry, R., and Dalbey, R.E. (2003). The Alb3/Oxa1/YidC protein family: Membrane-localized chaperones facilitating membrane protein insertion? Trends Cell Biol. **13,** 510–516.

Laemmli, U.K. (1970). Cleavage of structural proteins during the assembly of the head of bacteriophage T4. Nature **227,** 680–685.

Mori, H., and Cline, K. (2001). Post-translational protein translocation into thylakoids by the Sec and DeltapH-dependent pathways. Biochim. Biophys. Acta **1541,** 80–90.

Moore, M., Goforth, R.L., Mori, H., and Henry, R. (2003). Functional interaction of chloroplast SRP/FtsY with the ALB3 translocase in thylakoids: Substrate not required. J. Cell Biol. **162,** 1245–1254.

Moore, M., Harrison, M.S., Peterson, E.C., and Henry, R. (2000). Chloroplast Oxa1p homolog albino3 is required for post-translational integration of the light harvesting chlorophyll-binding protein into thylakoid membranes. J. Biol. Chem. **275,** 1529–1532.

Nickelsen, J., Fleischmann, M., Boudreau, E., Rahire, M., and Rochaix, J.-D. (1999). Identification of *cis*-acting RNA leader elements required for chloroplast *psbD* gene expression in *Chlamydomonas*. Plant Cell **11,** 957–970.

Nilsson, R., Brunner, J., Hoffman, N.E., and van Wijk, K.J. (1999). Interactions of ribosome nascent chain complexes of the chloroplast-encoded D1 thylakoid membrane protein with cpSRP54. EMBO J. **18,** 733–742.

Park, H., and Hoober, J.K. (1997). Chlorophyll synthesis modulates retention of apoproteins of light-harvesting complex II by the chloroplast in *Chlamydomonas reinhardtii*. Physiol. Plant **101,** 135–142.

Polle, J.E., Benemann, J.R., Tanaka, A., and Melis, A. (2000). Photosynthetic apparatus organization and function in the wild type and a chlorophyll b-less mutant of *Chlamydomonas reinhardtii*. Dependence on carbon source. Planta **211,** 335–344.

Rutherford, A.W., Crofts, A.R., and Inoue, Y. (1982). Thermoluminescence as a probe of photosystem II photochemistry. The origin of the flash-induced glow peaks. Biochim. Biophys. Acta **682,** 457–465.

Schagger, H., and von Jagow, G. (1991). Blue native electrophoresis

for isolation of membrane protein complexes in enzymatically active form. Anal. Biochem. **199,** 223–231.

Schleiff, E., and Klosgen, R.B. (2001). Without a little help from 'my' friends: Direct insertion of proteins into chloroplast membranes? Biochim. Biophys. Acta **1541,** 22–33.

Serek, J., Bauer-Manz, G., Struhalla, G., van den Berg, L., Kiefer, D., Dalbey, R., and Kuhn, A. (2004). Escherichia coli YidC is a membrane insertase for Sec-independent proteins. EMBO J. **23,** 294–301.

Shen, G., and Vermaas, W.F. (1994). Chlorophyll in a *Synechocystis sp*. PCC 6803 mutant without photosystem I and photosystem II core complexes. Evidence for peripheral antenna chlorophylls in cyanobacteria. J. Biol. Chem. **269,** 13904–13910.

Sundberg, E., Slagter, J.G., Fridborg, I., Cleary, S.P., Robinson, C., and Coupland, G. (1997). ALBINO3, an *Arabidopsis* nuclear gene essential for chloroplast differentiation, encodes a chloroplast protein that shows homology to proteins present in bacterial membranes and yeast mitochondria. Plant Cell **9,** 717–730.

Swiatek, M., Kuras, R., Sokolenko, A., Higgs, D., Olive, J., Cinque, G., Muller, B., Eichacker, L.A., Stern, D.B., Bassi, R., Herrmann, R.G., and Wollman, F.A. (2001). The chloroplast gene *ycf9* encodes a photosystem II (PSII) core subunit, PsbZ, that participates in PSII supramolecular architecture. Plant Cell **13,** 1347–1367.

Tanaka, A., Ito, H., Tanaka, R., Tanaka, N.K., Yoshida, K., and Okada, K. (1998). Chlorophyll a oxygenase (CAO) is involved in chlorophyll b formation from chlorophyll a. Proc. Natl. Acad. Sci. USA **95,** 12719–12723.

Tu, C.J., Schuenemann, D., and Hoffman, N.E. (1999). Chloroplast FtsY, chloroplast signal recognition particle, and GTP are required to reconstitute the soluble phase of light-harvesting chlorophyll protein transport into thylakoid membranes. J. Biol. Chem. **274,** 27219–27224.

van Kooten, O., and Snel, J.F.H. (1990). The use of chlorophyll fluorescence nomenclature in plant stress physiology. Photosynth. Res. **25,** 147–150.

Vass, I., and Inoue, Y. (1992). Thermoluminescence in the study of photosystem II. In The Photosystems, Structure, Function and Molecular Biology, J. Barber, ed (Amsterdam: Elsevier), pp. 259–294.

Zhang, L., Paakkarinen, V., Suorsa, M., and Aro, E.M. (2001). A SecY homologue is involved in chloroplast-encoded D1 protein biogenesis. J. Biol. Chem. **276,** 37809–37814.